Available online at www.sciencedirect.com

ScienceDirect

IFAC Papers Online CONFERENCE PAPER ARCHIVE

IFAC PapersOnLine 54-21 (2021) 121–126

Towards an Access Economy Model for Industrial Process Control: A Bulk Tailings Treatment Plant Case Study

L.L. Rokebrand * **J.J. Burchell**[*,**] **L.E. Olivier**[*,***] **I.K. Craig** *

* *Department of Electrical, Electronic and Computer Engineering, University of Pretoria, Pretoria, South Africa.*
** *Sibanye-Stillwater Platinum, Middelkraal Farm, Marikana, 0284, South Africa.*
*** *Analyte Control, Pretoria, South Africa.*

Abstract: A nonlinear model for the surge tank of Sibanye-Stillwater's Platinum tailings treatment plant is derived and linearised. Three controllers (two classical feedback and one model predictive controller (MPC)) are presented for control of the plant, and it is shown that a decoupled proportional-integral (PI) control structure, as would be employed in practice, performs the worst, while a nonlinear MPC controller provides the best performance. To illustrate an access economy model concept for industrial process control, a cloud platform to facilitate the competition between various controllers is presented and a scenario given with the three controllers competing to control the surge tank process. The platform is shown to provide the plant access to a controller that performs better than what is available locally.

Keywords: dynamic modelling, simulation, process control, competing controllers, cloud platform, minerals processing

1. INTRODUCTION

With the move to an access economy based model in many industries, a similar shift in the field of industrial automation will likely follow (Eckhardt and Bardhi, 2015). There has in fact been a shift to moving the upper layers of the automation hierarchy away from the plant and into a cloud based service (Gershon (2013); Hegazy et al. (2017)). Industrial automation vendors are increasingly providing software and managed services, with many automation vendors having developed their own IIoT cloud platforms (Isaksson et al. (2018);O'Brien et al. (2019)).

A cloud platform is therefore proposed where a 'selector' evaluates a number of different controllers over a period of time, and at the end of each period, selects and implements the controller which has been determined optimal based on some performance measure. This philosophy would allow for a number of vendors to develop a control strategy for a particular plant $\mathbf{G}_p$ with the best performing controller, as determined by the selector, being chosen for control. This could allow for more competition in the industrial automation industry where a few large vendors typically dominate the market. The selector performance measure could be influenced by the price and complexity of the vendor controllers. In addition, users might impose other criteria, such as a performance and reliability rating, on the pool of possible vendors. Fig. 1 shows the feedback loop diagram of the proposed philosophy.

There are a number of issues that will need to be addressed and clarified in order for such a platform to be practically viable. These would include:

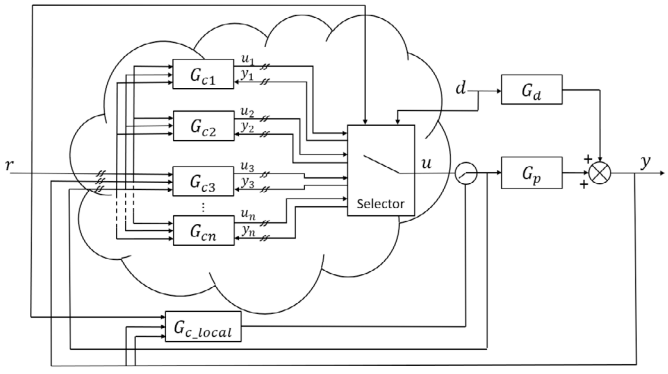

Fig. 1. Competing cloud platform controllers with a local fall-back controller.

(1) A process model would be needed for the development of each controller, and would thus have to be made available by the plant to each vendor (possibly via the selector) willing to compete to control the plant. The model could also be developed by the vendor from plant input-output data.
(2) Manipulated and controlled variable (MV and CV) constraints should be made available to the selector and the competing controllers for preventing the implementation of control moves which violate the constraints, and for use in controller development.
(3) The control actions provided by each controller should be simulated on a plant model in order to evaluate their performance. Such an evaluation is easy to do for reference following as long as the desired reference is available to the selector. This process is more

10.1016/j.ifacol.2021.12.021

challenging when evaluating the disturbance rejection capabilities of the competing controllers, as it will require some knowledge of the actual disturbances $\mathbf{d}$, either measured or estimated.

(4) The competing controllers are continuously evaluated in simulation on a plant model. When one of them is selected to control the real plant, the control moves generated by the selected controller will likely not be equal to those of the actual plant, but may in fact differ substantially. A bump-less transfer mechanism should therefore be used by each selected controller. Such a mechanism should know what the current plant control moves are, and when the controller switching is to take place.

(5) The idea is that the competing controllers reside in the cloud which could be remote from the actual plant to be controlled. A local controller is therefore required as a fall-back controller should a technical fault occur. Such faults could be local and/or include unreliable communication between the plant being controlled and the cloud platform on which the competing controllers reside. By the very nature of the requirements placed on this controller, it is necessary that it be locally installed at the plant. Controllers $\mathbf{G}_{c1}, \mathbf{G}_{c2}...\mathbf{G}_{cn}$ in Fig. 1 would typically be supervisory Advanced Process Controllers (APCs). A local base layer control infrastructure is assumed.

This paper presents a case study of the proposed control structure using a surge tank from Sibanye-Stillwater's Platinum bulk tailings treatment (BTT) plant, the aim of which is to keep the density of the tank outflow constant while maintaining a steady tank level. The dynamic model of the system is derived and linearised in Section 2. Section 3 presents three different controllers, two classical feedback and one MPC controller, and Section 4 presents the scenario where the three controllers compete to control the process via the cloud platform with the selector selecting the one it deems the best.

2. SURGE TANK DYNAMIC MODELLING

2.1 Model Derivation

A BTT surge tank is shown in Fig. 2. The input flow rate, the water flow rate, and the output flow rate are q_i, q_w, and q_o respectively. The input density, the density in the tank, and the output density are ρ_i, ρ, and ρ_o respectively. v represents the tank volume as calculated from a tank level measurement. A mass balance can be used to derive a dynamic surge tank model as

$$\frac{d\rho v}{dt} = \rho_i q_i + q_w - \rho_o q_o. \tag{1}$$

Perfect mixing is assumed such that the density in the tank is equal to the output density. (1) can then be simplified as

$$v\frac{d\rho}{dt} + \rho\frac{dv}{dt} = \rho_i q_i + q_w - \rho q_o. \tag{2}$$

The volume in the surge tank will be conserved if it is assumed that there is no volume change during mixing (Dontsov and Perice, 2014). This yields

$$\frac{dv}{dt} = q_i + q_w - q_o. \tag{3}$$

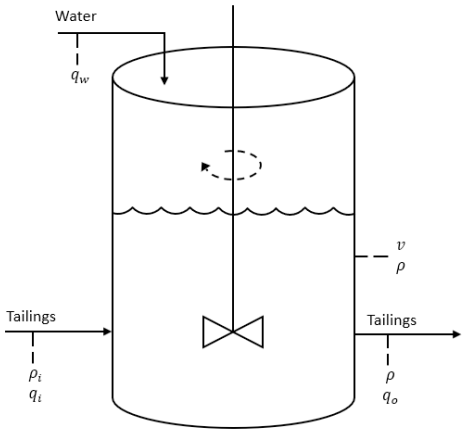

Fig. 2. BTT surge tank.

Substituting (3) into (2) gives

$$v\frac{d\rho}{dt} = \rho_i q_i + q_w - \rho(q_i + q_w). \tag{4}$$

The following non-linear state-space model can be obtained from (3) and (4):

$$\begin{bmatrix}\dot{v}\\ \dot{\rho}\end{bmatrix} = \begin{bmatrix} q_i + q_w - q_0 \\ \frac{1}{v}(\rho_i q_i + q_w - \rho(q_i + q_w))\end{bmatrix} \tag{5}$$

The system states are v and ρ, the inputs are q_i, q_w and q_o and the disturbance variable is ρ_i.

2.2 Model Linearisation

Applying a first order Taylor series approximation to (5) under equilibrium conditions yields the linear state-space model given by:

$$\begin{bmatrix}\delta\dot{v}\\ \delta\dot{\rho}\end{bmatrix} = \begin{bmatrix} 0 & 0 \\ -\frac{1}{v^2}(\rho_i q_i + q_w - \rho(q_i + q_w)) & -\frac{1}{v}(q_i + q_w)\end{bmatrix}^* \begin{bmatrix}\delta v\\ \delta\rho\end{bmatrix} + \begin{bmatrix} 1 & 1 & -1 \\ \frac{1}{v}(\rho_i - \rho) & \frac{1}{v}(1-\rho) & 0\end{bmatrix}^* \begin{bmatrix}\delta q_i\\ \delta q_w\\ \delta q_0\end{bmatrix} + \begin{bmatrix}0\\ \frac{q_i}{v}\end{bmatrix}^* \delta p_i \tag{6}$$

Table 1 show the nominal values of all the system variables obtained from historical data along with maximum and minimum values. Substitution of these values into (5) yields zero for the time derivatives of both v and p, confirming that these conditions constitute an equilibrium. Substitution of these values into (6) yields:

$$\begin{bmatrix}\dot{x}_1\\ \dot{x}_2\end{bmatrix} = \begin{bmatrix}0 & 0\\ 0 & -75\end{bmatrix}\begin{bmatrix}x_1\\ x_2\end{bmatrix} + \begin{bmatrix}1 & 1\\ 0.01 & -0.04\end{bmatrix}\begin{bmatrix}u_1\\ u_2\end{bmatrix} + \begin{bmatrix}0\\ 60\end{bmatrix} d \tag{7}$$

and

$$\begin{bmatrix}y_1\\ y_2\end{bmatrix} = \begin{bmatrix}1 & 0\\ 0 & 1\end{bmatrix}\begin{bmatrix}x_1\\ x_2\end{bmatrix} \tag{8}$$

The elements of the state vector $\mathbf{x}$ are ρ and v, the inputs $\mathbf{u}$ are q_i and q_w and the disturbance d is ρ_i. In this process the output flow rate q_o is kept constant, reducing the number of inputs to two. Converting (7) to a transfer function matrix model of the form:

$$\mathbf{y} = \mathbf{G}_p(s)\mathbf{u} + \mathbf{G}_d(s)d \tag{9}$$

yields:

$$\begin{bmatrix} y_1 \\ y_2 \end{bmatrix} = \begin{bmatrix} \frac{1}{s} & \frac{1}{s} \\ \frac{0.01}{s+75} & \frac{-0.04}{s+75} \end{bmatrix} \begin{bmatrix} u_1 \\ u_2 \end{bmatrix} + \begin{bmatrix} 0 \\ \frac{60}{s+75} \end{bmatrix} d \quad (10)$$

where the outputs y_1 and y_2 are equal to the states x_1 and x_2 or v and ρ respectively.

Table 1. Process variable nominal values and constraints

Variable	Nominal	Minimum	Maximum	Unit
v	10	3	20	m^3
ρ	1.4	1	1.5	$tonne/m^3$
q_i	600	300	1200	$m^3/hour$
q_w	150	0	750	$m^3/hour$
ρ_i	1.5	1	2	$tonne/m^3$

Perfect disturbance rejection is not possible for this process. This can be intuitively deduced from the system constraints given in Table 1. The disturbance variable ρ_i can vary between 1 and 2 $tonne/m^3$, thus if the set-point for the density ρ is fixed at the nominal value of 1.4 $tonne/m^3$, it will not be possible to maintain this density if the density of the feed falls below 1.4 $tonne/m^3$. If the input density increases to its maximum value of 2 $tonne/m^3$, it is possible to maintain the output density constant by decreasing the feed flow rate q_i to its lower constraint and increasing the water flow rate to 450 $m^3/hour$.

3. CONTROL PHILOSOPHIES

Three different controllers are presented which will be used in the competitive control scenario. This includes two classical feedback controllers, namely a de-coupled PI controller with the Skogestad Internal Model Control (SIMC) tuning and an ideal inverse controller, along with a non-linear MPC controller. These three controllers are denoted as $\mathbf{G}_{c\_local}$, $\mathbf{G}_{c1}$ and $\mathbf{G}_{c2}$ respectively (see Fig. 1).

3.1 Feedback Control

$\mathbf{G}_{c\_local}$ - *De-coupled PI Controller with SIMC Tuning:* De-coupled PI controllers tuned according to the SIMC rules (Skogestad, 2003) are used as the local fall-back controller as this is relatively easy for plant personnel to implement in practice. For the plant model in (10), the relative gain array (RGA) is found to be:

$$RGA(\mathbf{G}_p) = \begin{bmatrix} 0.8 & 0.2 \\ 0.2 & 0.8 \end{bmatrix} \quad (11)$$

over all frequencies. The diagonal elements are closer to one than the off-diagonal elements, thus for decentralised control, it is best to use the input flow rate q_i to control the tank volume v and the water flow rate q_w to control the liquid density ρ (Skogestad and Postlethwaite, 2005). Applying the SIMC rules in (Skogestad, 2003) to the models $\mathbf{G}_p(1,1)$ and $\mathbf{G}_p(2,2)$ in (10) for each input-output pairing, the following controller is derived:

$$\mathbf{G}_{c\_local} = \begin{bmatrix} \frac{100(s+25)}{s} & 0 \\ 0 & \frac{-2500(s+75)}{s} \end{bmatrix} \quad (12)$$

The tuning factor τ_c in (Skogestad, 2003) serves as a tuning parameter to adjust the aggressiveness of the controller. A value of 0.01 was chosen which corresponds with a 100 $rad/hour$ bandwidth.

Fig. 3 shows the response of the controller to an increase of 0.1 $tonne/m^3$ in ρ_i. The response of this controller is reasonable with respect to both tank volume v and density ρ with relatively small deviations from the set-point resulting from the disturbance.

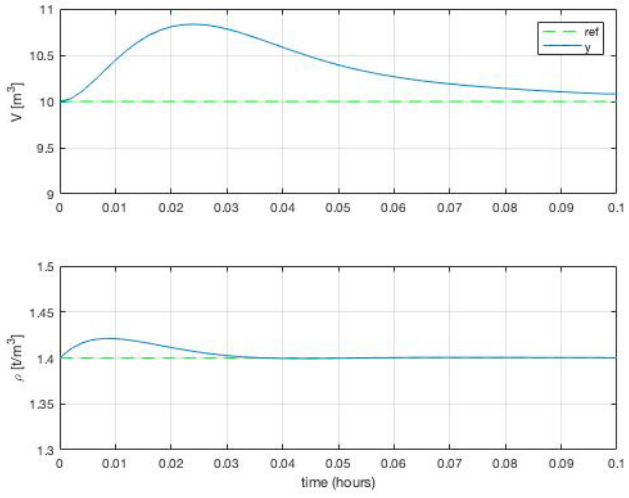

Fig. 3. Outputs of de-coupled PI controller $\mathbf{G}_{c\_local}$ for step disturbance of 0.1 $tonne/m^3$ in ρ_i.

$\mathbf{G}_{c1}$ - *Ideal Inverse Controller:* Ideal control is achieved by using the inverse of the plant model and is found to be:

$$\mathbf{G}_{c1} = \frac{k}{s}\mathbf{G}_p^{-1} = k \begin{bmatrix} 0.8 & \frac{20(s+75)}{s} \\ 0.2 & \frac{-20(s+75)}{s} \end{bmatrix} \quad (13)$$

where k is an adjustable gain parameter used to adjust the bandwidth of the controller. It can be seen that the resulting controller consists of two purely proportional elements and two elements which take on a PI structure, with the proportional elements acting only on the volume error and the PI elements acting only on the density error. The value of k was chosen to be 100, which yields a theoretical bandwidth of 100 $rad/hour$, same as that chosen for $\mathbf{G}_{c\_local}$. Fig. 4 which shows the response of the controller to an increase of 0.1 $tonne/m^3$ in ρ_i, simulated on the non-linear plant model given in (5). It can be seen that there is a steady-state offset in the tank volume V as result of the plant model mismatch and the purely proportional terms in the controller in (13) acting on this error. It can also be seen from this figure that the response in the density ρ is comparable with that of $\mathbf{G}_{c\_local}$.

3.2 $\mathbf{G}_{c2}$ Model Predictive Control (MPC)

An MPC controller ($\mathbf{G}_{c2}$) was designed using the state-space formulation of Mayne and Rawlings (2009) and the nonlinear model to perform predictions. A quadratic objective function given by:

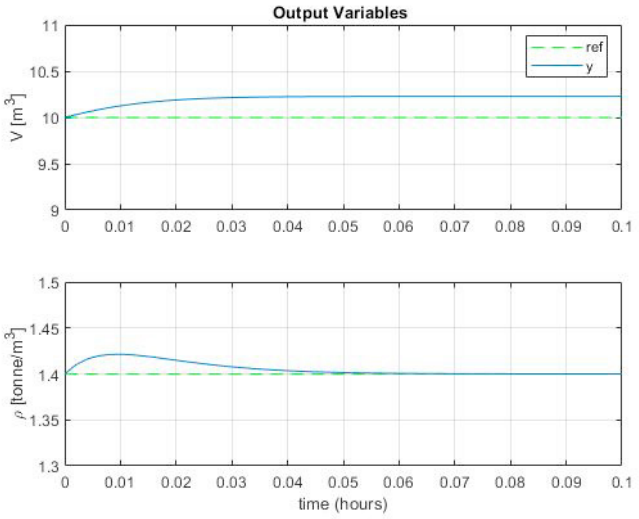

Fig. 4. Outputs of inverse controller $\mathbf{G}_{c1}$ for step disturbance of 0.1 $tonne/m^3$ in ρ_i.

$$V(\mathbf{u}, \mathbf{x}, \boldsymbol{\delta}, \mathbf{r}(k)) = \sum_{j=1}^{N_p} (\mathbf{r}(k) - \hat{\mathbf{y}}(k+j|k))^T \mathbf{Q} (\mathbf{r}(k) - \hat{\mathbf{y}}(k+j|k)) + \sum_{i=1}^{N_c} \Delta\mathbf{u}(i+k|k)^T \mathbf{R} \Delta\mathbf{u}(i+k|k) + \boldsymbol{\delta}(k)^T \boldsymbol{\Psi} \boldsymbol{\delta}(k) \quad (14)$$

was used, where k is the present sampling time, $\mathbf{x}(k) = \mathbf{y}(k) = [v, \rho]^T$ is the current state of the plant, $\mathbf{r}(k)$ is the reference or setpoint, $\hat{y}(k+j|k)$ is the predicted plant value at time $k+j$, $\boldsymbol{\delta}$ is the slack variable for constraint handling and N_c and N_p are the prediction and control horizons respectively. The weighting matrices $\mathbf{Q}$ and $\mathbf{R}$ used to tune the controller and the slack variable weighting matrix $\boldsymbol{\Psi}$ were chosen to be:

$$\mathbf{Q} = \begin{bmatrix} 1e-3 & 0 \\ 0 & 1 \end{bmatrix}, \quad \mathbf{R} = 0.25e-7 \times \mathbf{I}, \quad \boldsymbol{\Psi} = 1e7 \times \mathbf{I}$$

The error of the tank volume v thus contributes much less to the value of the objective function than the density ρ, with changes in the control action contributing the least in order to allow for more aggressive control action.

To account for plant model mismatch and unmeasured disturbances, additional states which serve as input disturbance estimates for each input were created and a linear Kalman Filter was used to provide estimates thereof, as described in Mayne and Rawlings (2009). The covariance matrices $\mathbf{Q}_w$ and $\mathbf{R}_n$ used in the synthesis of the Kalman Filter were chosen to be:

$$\mathbf{Q}_w = \mathbf{I}, \quad \mathbf{R}_n = 1e-5 \times \mathbf{I}$$

The larger the ratio between $\mathbf{Q}_w$ and $\mathbf{R}_n$, the more aggressive the observer and the quicker it will react to disturbances, thus the filter is tuned to be relatively aggressive.

The tuning parameters $\mathbf{Q}$, $\mathbf{R}$, $\mathbf{Q}_w$ and $\mathbf{R}_n$ were explicitly chosen to yield a response as similar as possible to that achieved in the ideal inverse controller, particularly in the density ρ.

Fig. 5 shows the response of the non-linear MPC controller to an increase of 0.1 $tonne/m^3$ in ρ_i.

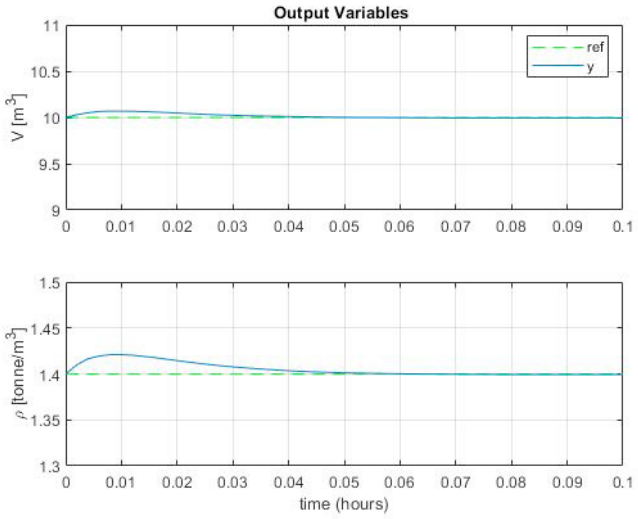

Fig. 5. Outputs of nonlinear MPC controller ($\mathbf{G}_{c2}$) for step disturbance of 0.1 $tonne/m^3$ in ρ_i.

4. COMPETING CONTROLLERS SCENARIO

This section presents a scenario where the controllers presented in Section 3 compete to control the actual plant as shown in Fig. 1. The disturbance d (the density of the feed ρ_i into the tank) is assumed to be perfectly estimated by the selector. The disturbance variable ρ_i varies between 1.74 $tonne/m^3$ and 1.35 $tonne/m^3$ over the 6-hour simulation period as shown in Fig. 6. The input density falls below the set-point of 1.4 $tonne/m^3$ about 3-hours into the simulation, for which time the set-point is unachievable.

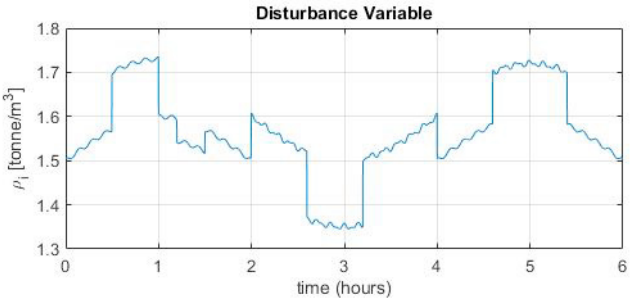

Fig. 6. Plant input density ρ_i acting as disturbance variable.

The selector evaluates the competing controllers by simulating them on the plant model over a particular evaluation horizon N_e. The sum of the squares of the error (SSE) in the simulated outputs is computed for each evaluation horizon as:

$$SSE_{tot} = \sum_{j=k-N_e+1}^{k} (\mathbf{r}(j) - \mathbf{y}_i(j))^T \mathbf{W}_e (\mathbf{r}(j) - \mathbf{y}_i(j)) \quad (15)$$

where $\mathbf{W}_e$ is a weighting matrix which is used to place more or less emphasis on the different outputs. At the

end of the evaluation horizon, the controller yielding the smallest value is deemed optimal and is selected. It is important for the plant model to be a good representation of the actual plant in order for the selector to work well.

As mentioned in point (4) of Section 1, a controller needs to initialise its output to correspond to the present control action implemented on the plant. This is deemed the responsibility of the controllers themselves. The MPC controller in this work achieve this by having two disturbance estimators, one which estimates the disturbances based on the measurement of the actual plant output and the actual control action implemented on the plant (both pieces of information which are available to the controllers), and a second which estimated the disturbance for the model it may be controlling. If one of the MPC controllers is selected, the disturbance estimate along with the actual plant measurements are used in the MPC optimisation algorithm and seamless transfer of control takes place. The classical feedback controllers employ a different principle in which the integral term of the controller is back initialised to yield a control action equal to that of the previous control action applied to the plant. This method successfully prevents the feedback controllers from generating any excessive control action in the event that control is switched over to them.

As is also mentioned in point (2) of Section 1, it is required that system constraints are supplied to the controllers. These constraints are incorporated in the MPC formulation described in Section (3), but there is no implicit constraint handling present in the classical feedback controller form. This is implemented ad-hoc by each controller by setting an output equal to its given constraint in the event that the output generated by the controller exceed this constraint. The other output is then set to its respective constraint, which is done to keep the tank level constant.

The evaluation horizon $\mathbf{N}_e$ should be chosen such that switching between controllers does not destabilise the closed-loop system. If the plant is exponentially stabilizable, as is usually the case for industrial systems, then the stability region of the closed-loop system will be an open and attractive set. If then a stabilizing supervisory controller is run for a finite but long enough time, it is possible for it to drive the process into this stability region. The switched system will therefore be stable as long as the intervals between switching are longer than the corresponding slowest individual closed loop system dynamics. For the purposes of the proposed platform this translates into a minimum bandwidth requirement for each competing controller. Therefore to ensure that the evaluation horizon $\mathbf{N}_e$ is much longer than the expected dynamics of the fastest closed-loop system, it was set to 30 minutes. The weighting matrix in (15) is chosen to be

$$\mathbf{W}_e = \mathbf{Q} = \begin{bmatrix} 1e-3 & 0 \\ 0 & 1 \end{bmatrix} \tag{16}$$

which is the same as the weighting matrix $\mathbf{Q}$ used in the performance index of the MPC controller, placing significantly more emphasis on the density ρ than the volume v.

Fig. 7 show the plant outputs and Fig. 8 the plant inputs for when the plant is controlled via the platform. The selected controller is shown in Fig. 9 over the 6-hour simulation period. The simulation of each controller, which is performed by the selector, is done on the nonlinear plant model. A 10% gain uncertainty is also applied to the input water flow-rate q_w of the actual plant. As

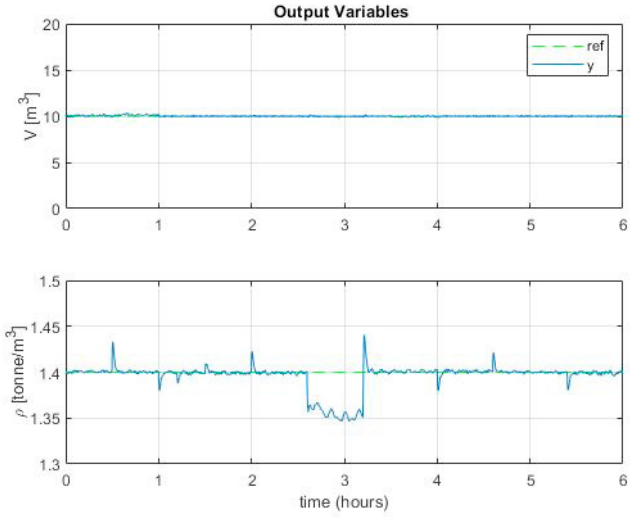

Fig. 7. Plant outputs under cloud platform control.

can be seen in Fig. 9, control is initially performed by the local controller $\mathbf{G}_{c\_local}$ (controller 0), which is the de-coupled PI controller, after which control is switched over to controller $\mathbf{G}_{c1}$ (controller 1). For the remainder of the simulation period, control is performed by $\mathbf{G}_{c2}$ (controller 2), which is the MPC controller, apart from a single evaluation period between 3.5 and 4 hours where the inverse controller $\mathbf{G}_{c1}$ was selected. This means that during the evaluation horizons between 0.5-1 hours and 3.5-4 hours, the inverse controller $\mathbf{G}_{c1}$ performed better in controlling the model than the MPC controller $\mathbf{G}_{c2}$.

In the period from 2.6 hours to 3.2 hours the set-point density of 1.4 $tonne/m^3$ is not achievable as the input density ρ decreases below 1.4 $tonne/m^3$ as can be seen in Fig. 6, hence the deviation from set-point in the output ρ.

In order to provide a quantitative measure of overall system performance, the sums of the squares of the error (SSE) over the whole simulation were calculated according to:

$$SSE_i = \sum_{k=1}^{N} (r(k) - y_i(k)) \cdot (r(k) - y_i(k)), \tag{17}$$

where N is the total number of samples in the simulation and the subscript i denotes the output (i.e. 1 for v and 2 for ρ). The sum of the squares of the error according to (17) achieved in the tank volume v and output density ρ with the cloud platform controller are 88 and 0.66 respectively. Table 2 shows the sum of the squares of the error according to (17) achieved in the tank volume v and output density ρ for each controller acting alone on the plant for the same disturbance scenario given in Fig. 6, as well as the total calculated according to (15) over the full 6 hours of simulation. It can be seen that the value achieved in the density ρ, when the plant is

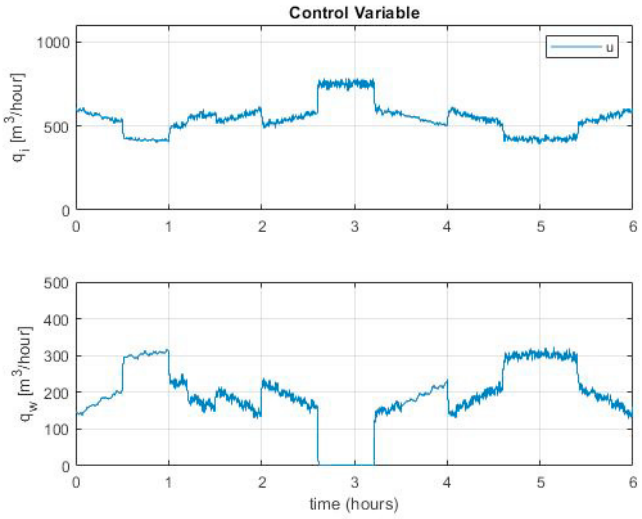

Fig. 8. Plant inputs under cloud platform control.

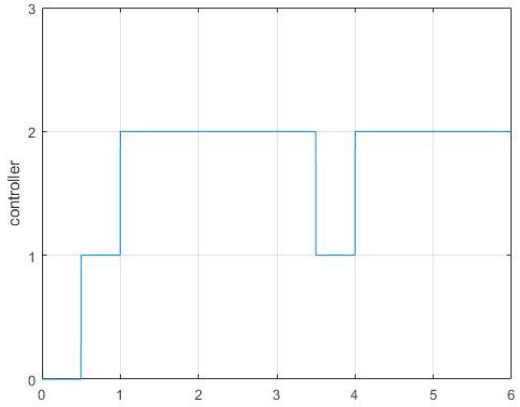

Fig. 9. 6-hour simulation showing the controller selected by the platform. Controller 0 is the local controller $\mathbf{G}_{c\_local}$, controller 1 is $\mathbf{G}_{c1}$, and controller 2 is $\mathbf{G}_{c2}$.

under platform control, is comparable with the individual controllers acting alone. The SSE for the volume v when the plant is under platform control, is much larger than for $\mathbf{G}_{c2}$, which is due to the initial selection of the decoupled PI controller $\mathbf{G}_{c\_local}$, which performs poorly in terms of level control. The MPC controller performs best in terms of level v and density ρ control. Given that the platform starts out with the suboptimal local controller $\mathbf{G}_{c\_local}$, the fact that it achieves a level of performance similar to that of the MPC controller, is notable.

Table 2. Controller performance indices with the platform and for each individual controller acting alone

	SSE_ρ	SSE_v	SSE_{tot}
No Platform ($\mathbf{G}_{c\_local}$)	0.66	490	1.15
With Platform	0.66	88.0	0.75
Inverse Controller ($\mathbf{G}_{c1}$)	0.66	168	0.83
NMPC Controller ($\mathbf{G}_{c2}$)	0.66	7.80	0.67

5. CONCLUSION

A detailed non-linear model of Sibanye-Stillwater's Platinum tailings treatment plant is derived. The model was subsequently linearised. Three controllers were presented for control of the plant: a local de-coupled PI controller, a simple inverse controller, and a nonlinear MPC controller. A cloud platform to facilitate the competition between various controllers was presented and a scenario given where the three controllers compete to control the surge tank process. It was shown that: 1) a simple de-coupled PI control structure, which would typically be employed on an industrial plant, performs relatively poorly, 2) that sufficient control can be achieved with the inverse controller which is probably the cheapest possible multivariable controller, and 3) the nonlinear MPC controller provided the best overall performance. The cloud platform, shown to perform similarly to the nonlinear MPC controller on its own, provides the plant with access to a controller that performs better than what is available locally. In addition, the platform could possibly provide a supervisory control solution at a lower cost than when locally employing a single solution such as the nonlinear MPC controller.

REFERENCES

Dontsov, E.V. and Perice, A.P. (2014). A new technique for proppant schedule design. *Hydraulic Fracturing Journal*, 1(3), 1-8.

Eckhardt, G.M. and Bardhi F. (2015) The Sharing Economy isn't About Sharing at All. online: https://hbr.org/2015/01/the-sharing-economy-isnt-about-sharing-at-all

Gershon, H. (2013). Control in the cloud: trends in cloud computing and their impact on the world of industrial control. online: http://emea.rockwellautomation.com/downloads/ Cloud%20Control

Hegazy, T., Abdelaal, A.E., Trsek H. and Hefeeda, M. (2017) Event-base control as a cloud service. *in Proc. 2017 American Control Conference*, Seattle, USA.

Isaksson, A.J., Harjunkoski, I. and Sand, G. (2018). The impact of digitalization on the future of control and operations. *Computers and Chemical Engineering*, 114, 122-129.

Mayne, D.Q. Rawlings, J.B. (2009) *Model Predictive Control: Theory and Design*, Nob Hill, Madison WI.

O'Brien, I., Polsonetti, C., Forbes, H., Guilfoyle, M. and Cosman, E. (2019). Top 50 Automation Companies of 2018: Are you ready to rumble? *Control Magazine*, October.

Skogestad, S. (2003). Simple analytic rules for model reduction and PID controller tuning, *Journal of Process Control*, 13(4), 291-309.

Skogestad, S. and Postlethwaite, I. (2005). *Multivariable Feedback Control: Analysis and Design*, John Wiley and Sons, 2nd edition.

Sontag, E.D. (1998). *Mathematical Control Theory: Deterministic Finite Dimensional Systems*, Springer, New York, 2nd edition.

Zhou, K. Doyle, J.C. Glover, K. (1995). *Robust and Optimal Control*, Prentice-Hall, New York.